Final Technical Report

Project Title: Clean Steel Casting Production

DOE Award Number: DE-FC36-04GO14230

Project Period: March 2005 – December 2013

Principal Investigators:

Selcuk Kuyucak, 905 645 0777, Selcuk.kuyucak@NRCan.gc.ca (2005 to 2007)

Delin Li, 905-645-0778, Delin.li@NRCan.gc.ca (2012 to 2013)

CanmetMATERIALS, Natural Resources Canada

183 Longwood Road South, Hamilton, ON, L8P 0A5, Canada

Formerly CANMET MTL (Materials Technology Laboratory),
Natural Resources Canada
568 Booth Street, Ottawa, ON, K1A 0G1, Canada

Participated Companies:

Harrison Steel Castings Co, Attica, Indiana

Wescast Industries Inc., Brantford, Ontario

December 31, 2013

Acknowledgment and Disclaimer:

Contents

List of Figures

List of Tables

1 Executive Summary

Inclusions in steel castings can cause rework, scrap, poor machining, and reduced casting performance, which can obviously result in excess energy consumption. Significant progress in understanding inclusion source, formation and control has been made. Inclusions can be defined as non-metallic materials such as refractory, sand, slag, or coatings, embedded in a metallic matrix. This research project has focused on the mold filling aspects to examine the effects of pouring methods and gating designs on the steel casting cleanliness through water modeling, computer modeling, and melting/casting experiments.

Early in the research project, comprehensive studies of bottom-pouring water modeling and low-alloy steel casting experiments were completed. The extent of air entrainment in bottom-poured large castings was demonstrated by water modeling. Current gating systems are designed to prevent air aspiration. However, air entrainment is equally harmful and no prevention measures are in current practice. In this study, new basin designs included a basin dam, submerged nozzle, and nozzle extension. The entrained air and inclusions from the gating system were significantly reduced using the new basin method.

Near the end of the project, there has been close collaboration with Wescast Industries Inc., a company manufacturing automotive exhaust components. Both computer modeling using Magma software and melting/casting experiments on thin wall turbo-housing stainless steel castings were completed in this short period of time. Six gating designs were created, including the current gating on the pattern, non-pressurized, partially pressurized, naturally pressurized, naturally pressurized without filter, and radial choke gating without filter, for Magma modeling. The melt filling velocity and temperature were determined from the modeling. Based on the simulation results, three gating designs were chosen for further melting and casting experiments on the same casting pattern using the lip pouring method. It was observed again that gating designs greatly influenced the melt filling velocity and the number of inclusion defects. The radial choked gating showed improvements in casting cleanliness and yield over the other gatings, even though no mold filters were used in the gating system.

2 Introduction

2.1 Introduction and Background

The manufacture of castings is one of the most challenging of technologies. This is because so much needs to be controlled simultaneously, including melting, alloying, molding, pouring, solidification, finishing, etc. Every one of these production steps has to be correct since failure of only one will probably cause the whole products to be unacceptable to the customer. Scrap or re-work due to inclusions cause a cost of up to 16% of the manufacturing costs for a typical metal caster. Significant progress in understanding casting inclusions has been made, including classifications, formation mechanisms, examples, and recommended prevention practices. For example, inclusion types can be classified into (1) exogenous and indigenous inclusions according to their source, (2) macroinclusions and microinclusions according to their size, or (3) blocky and linear inclusions according to their shape. Generally, if the inclusion is blocky, it is a sand-type inclusion. If it is linear, it is a dross-type inclusion. Mold filling has been identified as the most important step influencing entrainment defects such as extrinsic inclusions (slags, flux, refractory, sand, old oxides, and re-oxidation oxides), gas bubbles, mold erosion, and bi-films (folding-in of oxide films in liquid metal).

In bottom pouring operations, the high velocity metal stream can drag and entrain a considerable amount of air (on average 30% air by steel volume) as it impinges the metal surface in the pour basin. Conventional gating systems allow this air to be carried to the mold cavity and dissipate through the mold walls. The movement of both steel and hot gases through the gating system slows down the filling rate, generates a great deal of turbulence in the mold cavity which intensifies the radiation, and deteriorates the cope surface because of increased thermal load on sand. Sleeves with and without argon shrouding were used to isolate the metal stream from the surrounding air. These measures helped achieve cleaner steels with a 60-88% improvement reported in casting cleanliness. The method is suitable for large castings when the benefits outweigh the cost of its implementation.

In addition to the casting process, alloy types are a contributing factor for casting cleanliness. Carbon steels are more sensitive to formation of inclusions, re-oxidation, and gas porosity, as compared to high-alloy stainless steels. Deoxidation treatment of carbon steel is indispensable to produce clean castings. As much as 80% of the macroinclusions have been ascribed to re-oxidation in bottom-poured carbon steel castings. Deoxidation practice may not be required for stainless steel melts, because their high-Cr content may be sufficient for self-deoxidation. The mold filling of stainless steel castings can still greatly influence the formation of entrainment defects.

The purpose of this study was to minimize the casting surface defects through investigating the mold filling using water simulation, computer simulation, and melting/casting experiments. The initial stage of the research at Canmet's Ottawa laboratory was to complete a comprehensive mathematical model, water simulation, and carbon steel experiments using the bottom-pouring method. In addition, industrial trials at Harrison Steel, Attica, Indiana, were performed using the new designed basins and the trial castings were evaluated. The remaining stages of the project aimed at automotive turbo-housing stainless steel castings in the aspects of gating designs, flow simulation using Magma software, and melting/casting experiments. In this stage, work was completed in the new location of CanmetMaterials laboratory, Hamilton, Ontario, and in close collaboration with Wescast Industries Inc. Brantford, Ontario.

2.2 Specific Goals and Objectives

Goals and objectives were divided into a five specific tasks as follows:

TASK 1 – Research the current status of steel casting cleanliness. Current steel casting mold filling practices and steel casting inclusions were researched through a combination of literature search, industrial surveys, and data gathering in plant visits.

TASK 2 – Develop mathematical models and water simulation for the bottom-pouring. Following Task 1, the mathematical models and water modeling of the bottom-pouring systems were developed to investigate the air entrainment and turbulence in mold filling. The Reynold's number was used as a measure of turbulence and its relation to casting quality was investigated. Determine if there is critical [Re] for which mold erosion and reoxidation show a rapid increase. Study the effect of filtration. Use water modeling to visualize turbulence. New basins with a dam, submerged nozzle, and nozzle extension were designed to mitigate the air entrainment and turbulence using water model systems.

TASK 3 – Conduct melting/casting experiments to compare with simulation results. The results from Task 2 are used to design casting experiments at Canmet laboratory and Harrison Steel Company. Carbon steel plate castings were made in lab experiments, and large spindle castings for an off-road vehicle were made in the industrial trials. Determine the effect of mold filling time and mold quality on cope-side defects. Filling time was varied by casting thicker plates. Mold quality was varied by changing the molding media and mold preparation. Study the effectiveness of reflective coatings in reducing the heat absorption from radiation. Study the effect of soluble aluminum (strong deoxidizer) content in the metal on reoxidation and sand/metal reaction. The trial castings were visually inspected.

TASK 4 – Gating designs and flow simulation using Magma software. Small, thin-wall turbo-housing stainless steel castings for automotive applications were chosen to investigate the gating influences on the

mold filling using lip pouring method. Flow simulation using Magma software was performed on six gating designs to determine the filling temperature and velocity.

TASK 5 – Industrial trials of producing turbo-housing stainless steel castings. Based on the results obtained from Task 4, three gating designs were applied to the same casting pattern respectively for industrial melting/casting trials using the lip pouring method. Trial castings were evaluated and metallographic samples were taken for SEM analysis to characterize the inclusions.

2.3 Team Members

Dr. Selcuk Kuyucak created the original research proposal. He was the principal investigator and project leader in the first stage of the project from 2005 to 2007, completing the mathematical models, water simulations, carbon steel plate trials, and industrial trials.

Dr. Delin Li was the principal investigator and project leader in the second stage of the project from 2012 to 2013, collaborating with Wescast Industries Inc. to complete the flow modeling using Magma software and industry trials on automotive turbo-housing stainless steel castings. He is a research scientist of CanmetMaterials, and also had 13 years of manufacturing and R&D experiences in iron and steel casting industry (Wescast Industries Inc.). ASQ-certified Six Sigma Black Belt and ASQ CQE. He was a senior NRC associate in USA at Marshall Space Flight Center NASA, Huntsville, Alabama, and Alexander-von-Humboldt Fellow at German Aerospace Research Center, Cologne, Germany.

John Carpenter coordinated the industrial trials at Harrison Steel Company.

Wescast Industries Inc. also contributed to this project: computer simulations were performed by Carlos Amaral and Ashraf Pindari; melting and casting experiments were conducted by Nigel Heap, Doug Aitchison, and Alex Schoemaker; chemistry analyses were performed by Feila Yu; Clayton Sloss and Bartek Makarski coordinated the effort.

CanmetMaterials team members also included Renata Zavadil (micrographs) and Howard Webster (chemical analyses).

3 Results and Discussion

A summary of the research highlights is included in this final report by research task. The full publications (see list in Section 6.1) include more details from the research.

3.1 TASKS 1 – Research the Current Status of Steel Casting Cleanliness

3.1.1 Deoxidation and Formation of Inclusions

Steels are deoxidized to decrease their soluble oxygen content to a sufficiently low value to prevent CO-porosity. Sufficient deoxidizer is added to remove soluble oxygen in the form of indigenous oxide inclusions and to ensure that oxygen activity is less than 1-2 ppm at the moment of solidification. This is achieved by strong de-oxidizers, such as aluminum, whose soluble content at the moment of solidification must be at least 100-200 ppm. Aluminum reacts with soluble oxygen and the existing manganese silicates to produce alumina inclusions. The aluminum added must be sufficient to:

- stoichiometrically convert the oxygen in the steel melt to alumina
- allow for reoxidation losses
- allow for a minimum residual retained in solution at the moment of solidification

The total additions of aluminum for deoxidation varies between 0.06–0.12%. Recovery of aluminum in the final steel casting can vary from 30% to 60%, depending on the degree of reoxidation in process.

3.1.2 Reoxidation

Deoxidation renders steel active, reoxidation starts immediately and results in a loss of soluble aluminum. The degree of reoxidation depends on melt processing, in which pouring and mold filling are especially critical as large surface areas are exposed to the atmosphere. Even a standing steel melt in a small induction furnace loses aluminum to oxidation approximately exponentially, with a half-life of 4 minutes. Reoxidation was found to account for more than 80% of the macroinclusions. In bottom-pouring operations, nozzle sleeves or argon shrouding was used to prevent the metal stream being exposed to atmosphere.

3.1.3 Inclusion Separation

Inclusion chemistry plays a significant role in the way inclusions form and behave in a steel melt. Silica inclusions in silicon-killed steels tend to be compact in form, remain separate and have low removal rates. The less-wetting alumina inclusions, on the other hand, form branched dendrites, tend to coagulate into colonies and stick to free surfaces. For instance, during pouring from ladles, a heavy build-up of alumina inclusions occurs at the nozzle-entry area where metal streamlines converge and increase the chances of refractory – inclusion incidence. The build-up occurs in spite of the intuitively expected high shear forces in this area. This sticking tendency results in high removal rates, but also a high proportion of alumina macroinclusions in steel. In wrought steelmaking, Si-killed steel plates having 120 ppm oxygen are considered cleaner than Al-killed plates with 60 ppm oxygen, because of the much greater incidence of mac-

roinclusions (those greater than >40 µm) in the latter. Oxide inclusions extracted from steel samples by dissolving the metal matrix in acid, and suspending the particles in an aqueous media for sizing and counting in a Coulter Counter, show that greater than 10% of the total inclusion volume could be macroinclusions in Al-killed steels, but less than 1% in Si-Mn killed steels. Generally, inclusions that are not easily wetted by steel will behave like alumina to decrease their interfacial energy, although, the exact nature of the forces in play between particles or particles and free surfaces is not well understood.

3.1.4 Inclusion Modification

The detrimental effects of alumina inclusions can be mitigated to some extent by calcium additions. Calcium has very little solubility in steel, and is volatile at steelmaking temperatures. Its addition presents a technical challenge but the commercially available wire-injection equipment makes this a routine operation with good recoveries. Calcium's high affinity for oxygen can modify the alumina inclusions to low melting-point calcium aluminates. These are molten at steelmaking temperatures, and therefore, are spherical. Because of their compact shape, they present much less area as cope-side defects and are less harmful for machinability and mechanical properties.

3.1.5 Gating Practices and Cope-Side Defects

Mold filling has been identified as the most important factor affecting the cope-surface quality. In an SFSA initiated work, Harrison Steel looked at all aspects of their melting and casting procedures for a steel casting and finally identified a high gating ratio to be the most important in reducing the cope side defects. When gating ratio was increased from 1:1:1 to 1:3:3 from a bottom-pouring ladle, the "dirt length" went down from 12-40" to 2.2". Mold turbulence increased reoxidation and sand/metal reactions, and was the primary cause of cope-side defects in this casting configuration. Also, in large steel castings, increasing the pouring (mold filling) rate was observed to greatly improve the cope surface appearance. A number of hypotheses have been advanced for the formation of cope-side defects during filling: (a) macroinclusions float to the cope surface, (b) reoxidation on the free surface of metal, (c) cope sand expansion or reaction, and (d) exogenous inclusions. Experiments could be designed to test the significance of each one of these. The Harrison Steel work obtained a large improvement by changing the gating ratio. In bottom-pouring operations, it is desirable to keep the nozzle fully open. Therefore, the pouring rate varies with the metal height in the ladle. Because of the variable pouring rate, it is a common practice to have a large enough sprue to accommodate the maximum flow from a full ladle and not to choke the gating system. This is a significant cause for air entrainment. Some foundries are experimenting with a choked, tile-gate system with a sufficient sprue plus pouring basin height to allow for variations in the pouring rate.

The Reynold's number [Re] is a ratio of the inertial forces to viscous forces in fluid flow and determines the onset and the degree of turbulence in duct flow:

$$[Re] = \frac{VD}{\nu} \qquad \text{Eqn. 1}$$

where V is the average velocity across cross-section, D is the effective duct diameter, ν (nu) is the kinematic viscosity, (viscosity, μ / density, ρ), whose value for steel is 0.8-1.0 mm^2/s. With Reynold's numbers of less than 2000, the flow is laminar, while above 20,000 turbulence becomes severe. It is not practical to achieve laminar flow in gating systems, and the objective is to prevent severe turbulence by keeping the Reynold's number below 20,000. Filters, as flow-modifiers, also help reduce turbulence. Flow in the filter body is laminar because of the much reduced effective diameter. After the metal leaves the filter, the smooth flow continues, turbulence sets in gradually after a considerable distance in the runner. Filters for use in the gating system of steel castings are available commercially and have been tested with positive results. The kinematic viscosity of water at 1 mm^2/s is very close to that of steel, thus, the two fluids are said to have dynamic similarity. They will generate the same Reynold's numbers and similar turbulence when flowing in similar ducts under gravity. As a result, water has been used often to simulate and visualize steel flow in gating and mold filling studies.

3.1.6 Effect of Inclusions on Mechanical Properties

Second phase constituents affect the mechanical properties of alloys and the magnitude of this effect depends on their size, shape, distribution and interfacial properties. As oxide inclusions have very weak bonding with the steel matrix, they act almost like porosity. The most affected mechanical properties are ductility and fatigue strength. Unlike the grain boundary sulfide inclusions, oxide inclusions tend to randomly distribute themselves in steel, therefore, they are much less harmful to ductility. A steel casting having 0.02% O may be considered to have a higher than typical inclusion content, yet this amount corresponds to only 0.10 vol.% of oxide inclusions.

The strength-to-ductility ratio determines the notch sensitivity of a material. Oxide inclusions are not particularly detrimental in steel castings heat-treated to moderate strengths but become increasingly detrimental at higher strengths. In this respect, inclusion size and distribution are more important than the total content.

3.2 TASKS 2 – Developing Mathematical Models and Water Simulation for Bottom-Pouring

3.2.1 Mathematical Equations

Certain conditions must be met to realistically simulate one fluid with another. For an air entraining, plunging jet, we may consider imposing similarity on the inflow (impact) Froude's number [Fr_j], which is a ratio of inertial to gravity forces, and the Weber's number [We_j], a ratio of inertial to surface tension forces, which may be important in air bubble generation:

$$Fr_j = \frac{v_j^2}{g\,d_j}$$

Eqn 2

$$We_j = \frac{\rho_L\,v_j^2 d_j}{\sigma}$$

Eqn 3

For [Fr_j] similarity,
$$\frac{v_{j,W}^2}{d_{j,W}} = \frac{v_{j,Fe}^2}{d_{j,Fe}}$$

Eqn 4

For [We_j] similarity,
$$\frac{\rho_{Fe}\,v_{j,Fe}^2 d_{j,Fe}}{\sigma_{Fe}} = \frac{\rho_W\,v_{j,W}^2 d_{j,W}}{\sigma_W}$$

Eqn 5

where:

v_j jet velocity on impingement to free surface

d_j jet diameter on impingement to free surface

g acceleration due to gravity

ρ_L fluid density

σ fluid surface tension

w stands for water and Fe for steel. Collecting equations 4 and 5:

$$\frac{d_{j,W}}{d_{j,Fe}} = \sqrt{\frac{\sigma_W / \rho_W}{\sigma_{Fe} / \rho_{Fe}}}$$

Eqn 6

Table 1 shows the related fluid properties for steel and water. Substituting these into Eqn. 6:

$d_W = 0.52\,d_{Fe}$

$v_W = 0.72\,v_{Fe}$

$h_W = 0.52\,h_{Fe}$

$[Re]_W = 0.3\,[Re]_{Fe}$

Therefore, both Froude and Weber criteria are satisfied in water modeling if both the plunging steel jet diameter and the fluid head above the free-surface are halved. However, this half scale model will not satisfy the Reynold's criterion. The Reynold's number is a ratio of the inertial to viscous forces. It is used to establish the magnitude of drag forces, such as the terminal rise velocity of air bubbles; as well as the more commonly known criterion for the onset of turbulence in duct flow. A low [Re_j] in a half-scale water model will likely underestimate the residence time of entrained air; or conversely, in a full-scale steel process, the entrained air will tend to stay longer than what is visualized in a half scale water model. If air entrainment rates are similar, a half-scale water model can be used to conservatively simulate steel pouring operations.

Table 1 - Steel, water and air properties relevant to establishing similarity criteria

	Water	Steel	Air	
Temp. (°C)	20	1550	20	800
Density (kg/L)	1.0	7.0	1.18×10^{-3}	0.33×10^{-3}
Surf. tension (mJ/m^2)	71	1,870		
Viscosity (mPa s)	1.0	5.5	0.018	0.044
Z_c ($\times 10^{-6}$ m$^{1/2}$)	120	50		

Gas entrainment by plunging liquid jets in aqueous media:

$$R = \frac{Q_A}{Q_W} = 0.04 \, \mathrm{Fr}_j^{0.28} \left(\frac{L_j}{d_0} \right)^{0.4}$$
Eqn 8

where:

R entrainment ratio (volume of air per unit volume of liquid)

Q_A, Q_W volume flow rate of air and water

L_j jet length (free fall height of stream); d_0 nozzle diameter

For example, the expected air entrainment rate in water having a head height of 0.5 m, ladle nozzle diameter of 0.025 m (1 in.), and a free fall height of 0.2 m, is $R = 21$ pct. This is in good agreement with the previously measured entrainment rates of 15 – 60%. In addition, entrainment rate should increase with the square root of the air viscosity. If air in the vicinity of steel stream is 800 °C, its viscosity is twice as much as its room temperature value (Table 1), and this would cause a further 40 pct. increase in the entrained air volume.

3.2.2 Measurement of Entrained Air in Water Modeling

Figure 1 shows examples of air entrainment by a plunging jet in a reservoir of water. Although, both systems were similar in [Fr], [We] and [Re] criteria, the air entrainment behaviour was significantly different. The difference stemmed from the varying free-fall heights of the plunging jets (jet length L_j). Longer jet lengths increase the surface roughness of a stream through the action of air. In Figure 1(b), air bubbles were smaller, they were easily carried with the convective currents and their rise velocity was slower. The higher residence time of the bubbles led to an increase in the plume size even though less air was entrained.

A simple apparatus was built to measure the volume fraction of entrained air in the gating system of Figures 2 and 3. The entrained air/ water mixture was accumulated in a separation chamber, which had a baffle separating the air/water mixture from the air-free water. The baffle was open at the top and bottom to air and water, respectively; to equilibrate the water level on either side. On cue, water and air were accumulated in a tub and a plastic bag, respectively, for a timed period. The exit flow rate of water was controlled by squeezing a rubber hose connected to the end of acrylic tubing to ensure the level in separation chamber stayed the same during a measurement. Air entrainment rates varied between 20 and 60 pct., with an average entrainment rate of 30 pct. by water volume. Figure 2 shows a water modeling simulation of a bottom-pouring ladle into a "goose-neck" gating system built from acrylic materials. A spectacular amount of air becomes entrained and is carried into the mold cavity.
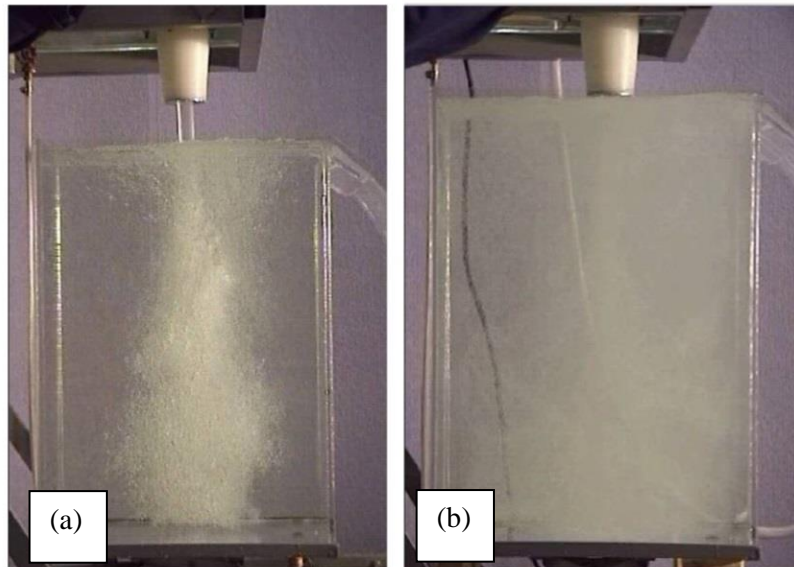

Figure 1 - Plunging jets from a 1" dia. nozzle to a water reservoir. The only difference between the two systems was the free-fall height of the jet: (a) 4" and (b) 1.75". Although, air entrainment by volume was greater in (a), smaller bubbles became entrained in (b), increasing the residence time of the plume.
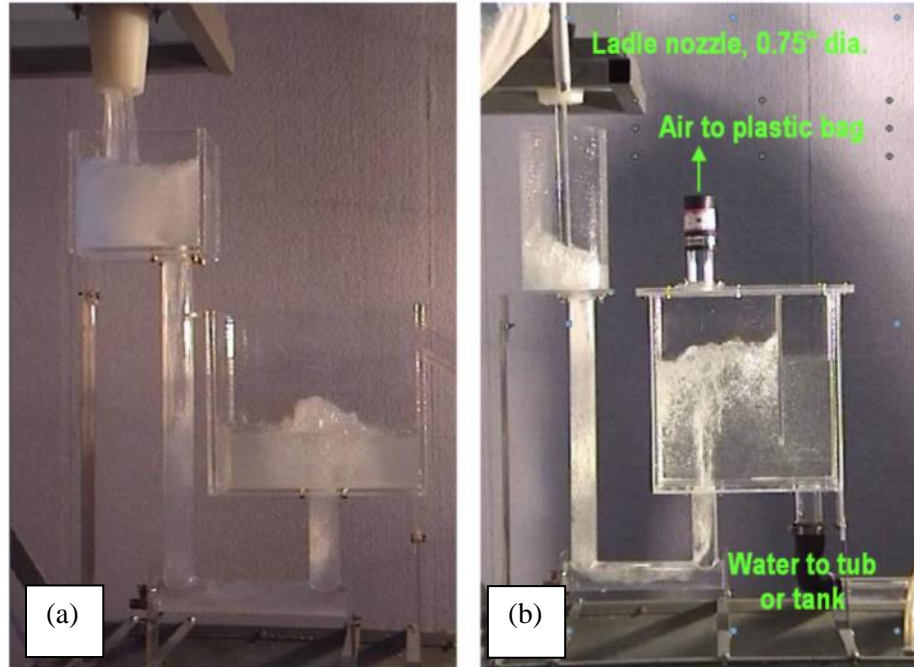
Figure 2 – Water modeling simulating goose-neck gating into a riser block with 1.5" dia. and 6" long ladle nozzle: (a) A spectacular amount of air became entrained, and (b) Apparatus measuring entrained air in a pouring cup. Entrained air / water mixture enters into a separation chamber through the same "goose-neck" gating system as Figure 2(a).

3.2.3 Developing Methods to Remove and Prevent Entrained Air

A pouring basin was used as an intermediary vessel to deal with the entrained air in a bottom-pouring ladle operation. Two approached were developed:

a. Use dams and weirs to divert the entrained air out of the pouring box,

b. Use a submerged nozzle extension from a bottom-pouring ladle to eliminate the entrrained air altogether.

The first method was the less expensive option. The second method provided a more complete solution to air entrainment. Shrouding methods have been used in the past. However, the compact size of a nozzle extension in the present case not requiring a large clearance made it more attractive, as it can be installed with the nozzle and carried with the ladle during tapping and pouring operations.

The ladle nozzle flow rate varies with the metal head height in the ladle, so a spreadsheet based flow model was developed in conjunction with the above methods that calculated and plotted the head heights in the ladle, pouring basin and the mold cavity with respect to pouring time, as shown in Figure 3. This

program was used to correctly size the pouring basin and gating dimensions to ensure that the pouring basin was kept compact without the risk of overflowing. Ideally, the metal in the pouring basin should rise up to a freeboard level and decrease as the ladle empties. These methods are currently suitable for a ladle pouring one large steel casting. The difficulty with multiple pours is gauging the end-pour time of the intermediate castings, as any remaining metal in the pouring basin may overflow the risers.

Numerous configurations of dams and weirs were tried in pouring basin water models built from acrylic materials. It was found that a single dam near the sprue inlet was sufficient to remove the entrained air (Figure 4a). In the absence of a dam, the major convective current sweeps the pouring basin floor (broken lines) and the entrained air gets caught in the down flow at the sprue inlet. The dam turns away this flow upwards, allowing entrained air to escape to the atmosphere before turning downwards again. A choke was placed to adjust the sprue diameter so water would accumulate in the pouring basin to allow for air separation. However, the pouring basin was undersized for the flow conditions from the ladle, and throttling was necessary to prevent overflow.

Figure 4b shows a larger pouring basin whose dimensions were checked by the flow model mentioned. As predicted, water rose to a maximum level in the pouring basin and then started to drop as the ladle emptied. In either case, excellent separation of entrained air was observed.

It was anticipated that once the nozzle is submerged, it would completely isolate the metal from air. However, two problems were encountered (Figure 5). There were a great deal of splashing on initial entry to the pouring basin and strong lateral convective currents entrained some air from the sides even after the nozzle became submerged. Various "splash guard" designs were considered to deal with the former problem. Typically, concave surfaces aggravated the problem, convex surfaces, like the back of a spoon, alleviated it. It was intended to break the impact of the falling stream and split it gently into divergent paths. Various cones and hemi-spherical surfaces were tried. The optimum pad was a semi-cylinder having a bell-shaped cross-section, placed in a well (Figure 5c). The semi-cylindrical pad split the stream primarily in the longitudinal directions, where there was more room; limiting the flow in the lateral directions, where circulation here caused air entrainment at the surface. A dam to divert the base convective current was not used in this design.

Studies in aqueous and organic systems indicate a much greater air entrainment in steels under similar conditions. Plume characterization such as bubble size distribution and plume penetration are also important in designing systems to adequately remove entrained air. It is desirable, therefore, to have direct visualization and measurement of entrained air in steels in limited cases by means of an x-ray study to establish a relationship between water modeling and actual steel processing with greater confidence.

Figure 3 – Flow model data entry for the bottom-pouring system.
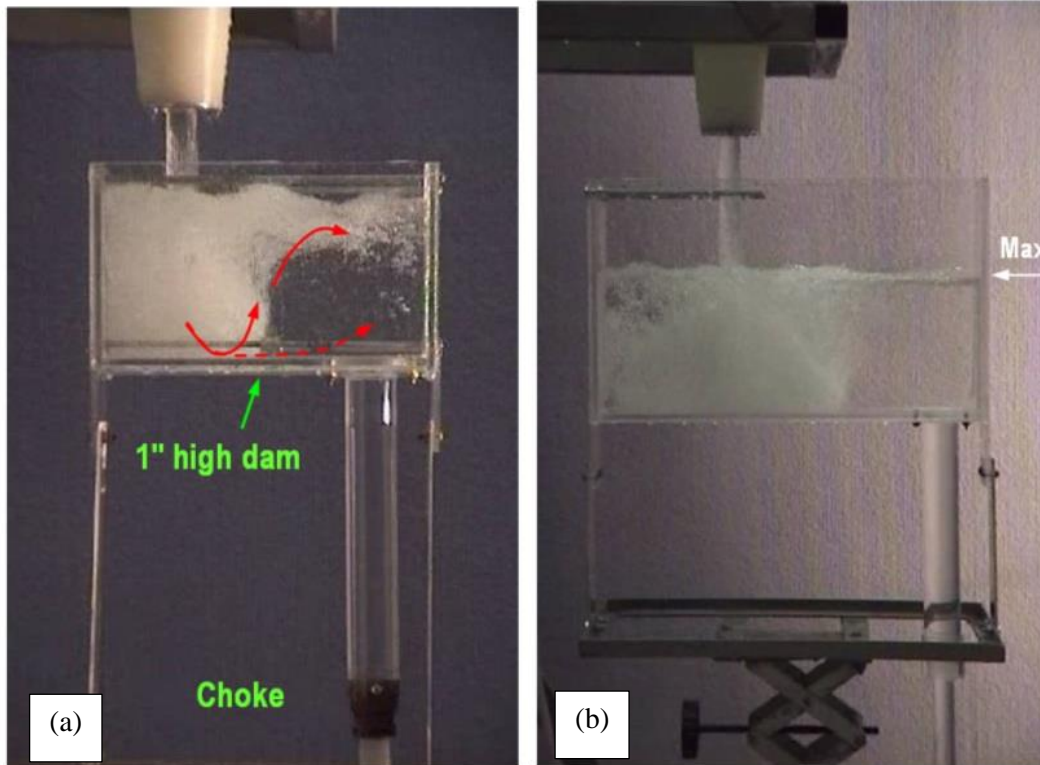
Figure 4 - Pouring basin with a single dam (a) dimensions: 1" dia. Ladle nozzle, 11" long, 6" high, 5" wide pouring basin, 1" high dam at 5" from right in pouring basin, 1½" dia. sprue with 1" dia. choke. (b) Larger pouring basin with a single dam. Dimensions: 1" dia. ladle nozzle, 18" long, 10" high, 5" wide pouring basin, 1" high dam at 6" from right in pouring basin, 1½" dia. sprue with 1.25" dia. choke.
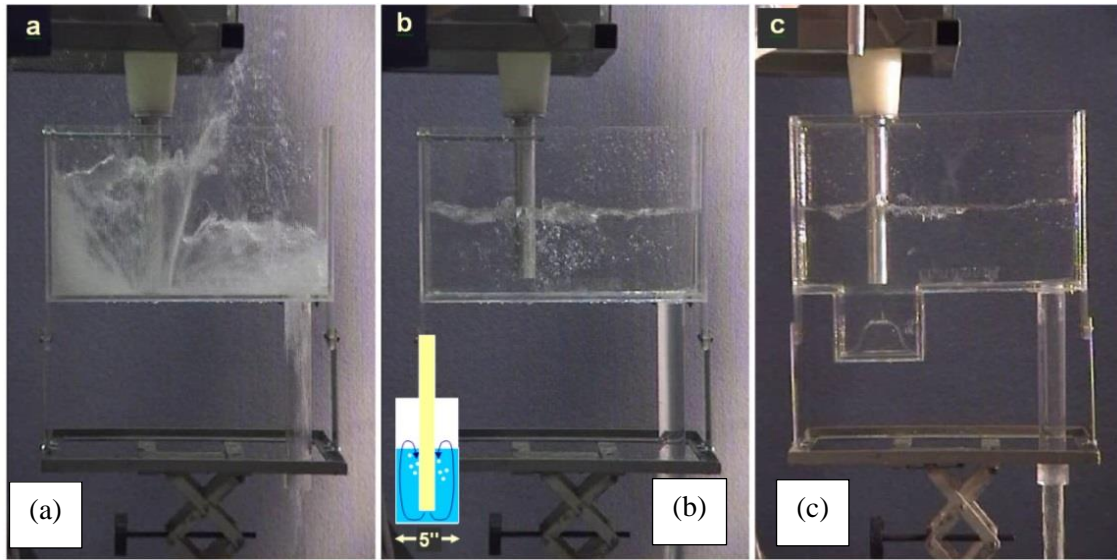
Figure 5 - Submerged ladle nozzle extension (nozzle extension is 1.125" dia., 10" long; other dimensions are the same as in Figure 3): (a) Splash on initial entry to pouring basin. (b) Submerged operation. Inset shows the lateral (width-wise) convection currents entraining air from the surface. (c) Operation with a splash guard installed in a pouring basin well.

3.3 TASKS 3 – Melting Casting Experiments to Compare with Simulation Results

3.3.1 Laboratory Experimental Procedures

Comparative wedge-block castings were made in AISI 1020 steel via a bottom-pouring ladle using a pouring cup or a pouring basin (Figure 6). Two wedge-blocks were poured from 440 kg heats, the first one utilizing a pouring cup (standard gating); and the second, a pouring basin with a dam, with or without a submerged nozzle extension (alternative gating). The second poured blocks with the alternative gating had a lower metal head in the ladle, but the ladle was raised to clear the pouring basin; thereby, decreasing the difference in pour heights between the two castings.

The molds were made in silica sand having an AFS grain size number of 55, bonded with 4.5 pct. by sand weight dextrin modified (5 pct.) sodium silicate (50 pct. aq.) binder. After removing the gates and risers, the castings were cleaned by sand blasting. Table 2 shows the experimental conditions and the results of cope-surface evaluation. Figures 7 and 8 show the cope surface photographs of the castings.

Manufacturers Standardization Society's Standard Procedure MSS SP-55 was used to distinguish which surface irregularities constituted a defect. A square inch grid was prepared on a transparent sheet and laid

over the cope surface. Each square on the grid incident on a defect and covered more than 2/3 by that defect was counted as one. If the square was only partially covered (1/3 to 2/3), a half score was given. The total score then was expressed as the "dirt count" of the cope surface.

3.3.2 Laboratory Experimental Results

The castings are shown in Figures 7 and 8. The review results were recorded Table 2. In all cases except the first one, cope-surface quality of the casting with the alternative gating was less satisfactory. The defects were mostly in the form of ripples, indicating a low temperature in the mold and premature freezing. The successful casting had the highest pour temperature. Effectively, the pouring basin as an intermediate vessel caused an additional heat loss, which needed to be compensated for. Therefore, conclusive statement cannot be made from Table 2, Figures 7 and 8.

Table 2 – Evaluation of cope-side defects in laboratory castings

Heat ID	Block ID	Pour (°C)	Nozzle Extension?	Cup or Basin	Dirt Count
F5071	A	1620	No	Cup	24
	B	1593	No	Basin & Dam	5
F5083	A	1591	Yes	Cup	8
	B	1577	Yes	Basin & Dam	16
F5085	A	1603	Yes	Cup	8
	B	1586	Yes	Basin & Dam	24
F5089	A	1603	No	Cup	9
	B	1583	No	Basin & Dam	20
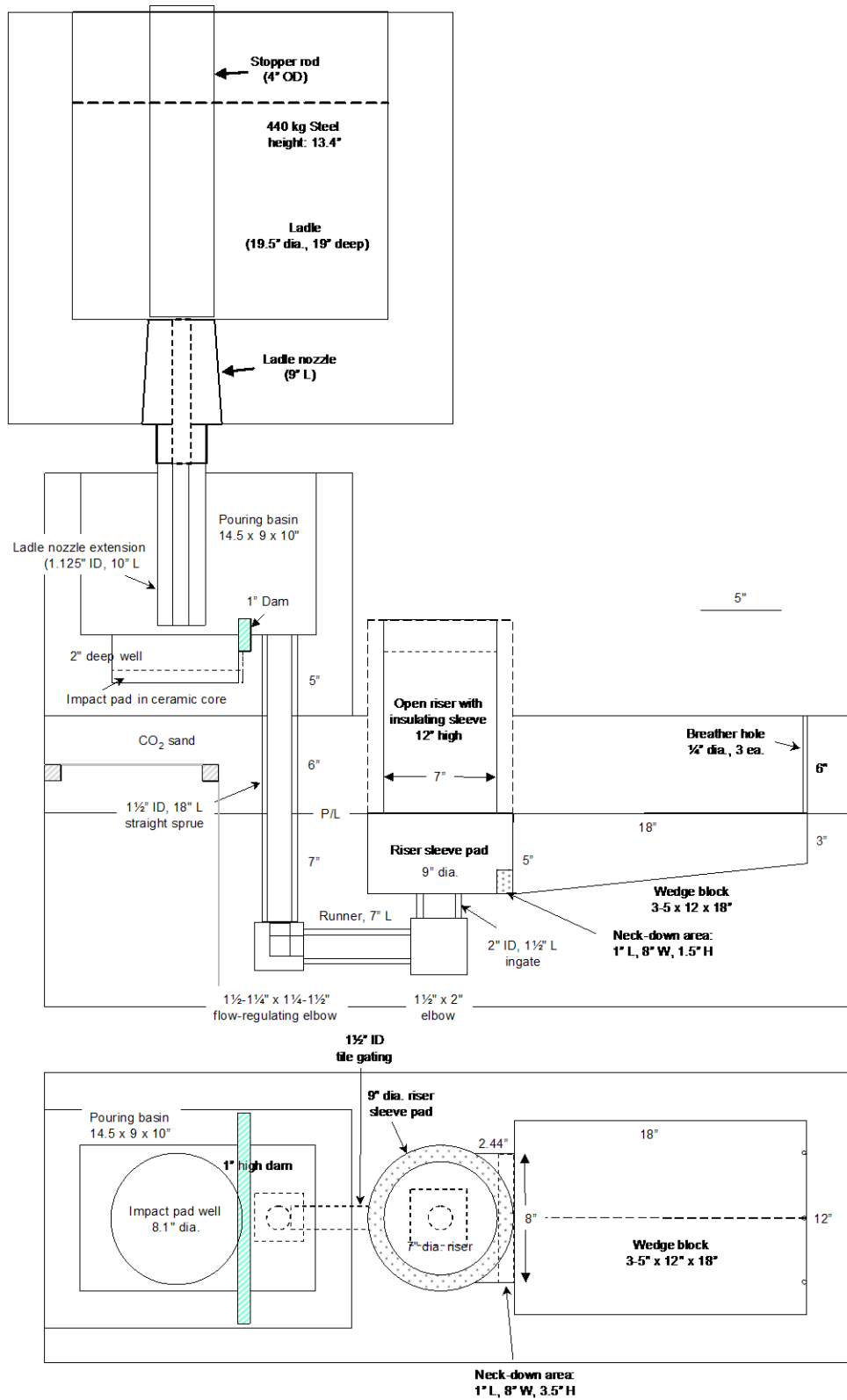
Figure 6 - Sketch of the wedge-block casting with a submerged ladle nozzle extension in pouring basin; side and plan views. Poured weight (with pouring basin): 225 kg, casting weight: 99 kg.

| F5071-A | F5071-B |
| F5083-A | F5083-B |
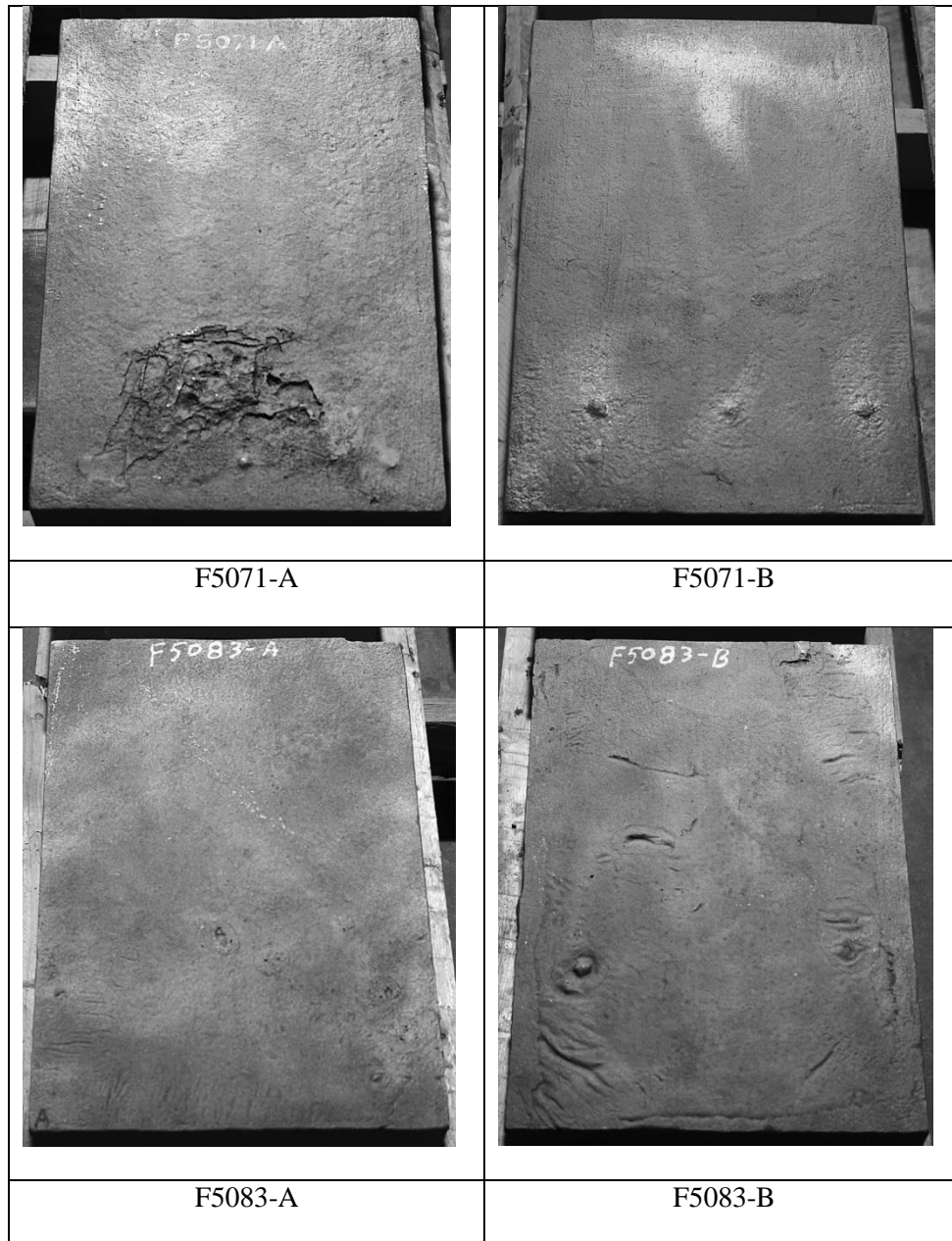
Figure 7 – Laboratory trials castings of heats F5071 and F5083. AISI 1020 carbon steel was poured.

F5085-A	F5085-B
F5089-A	F5089-B
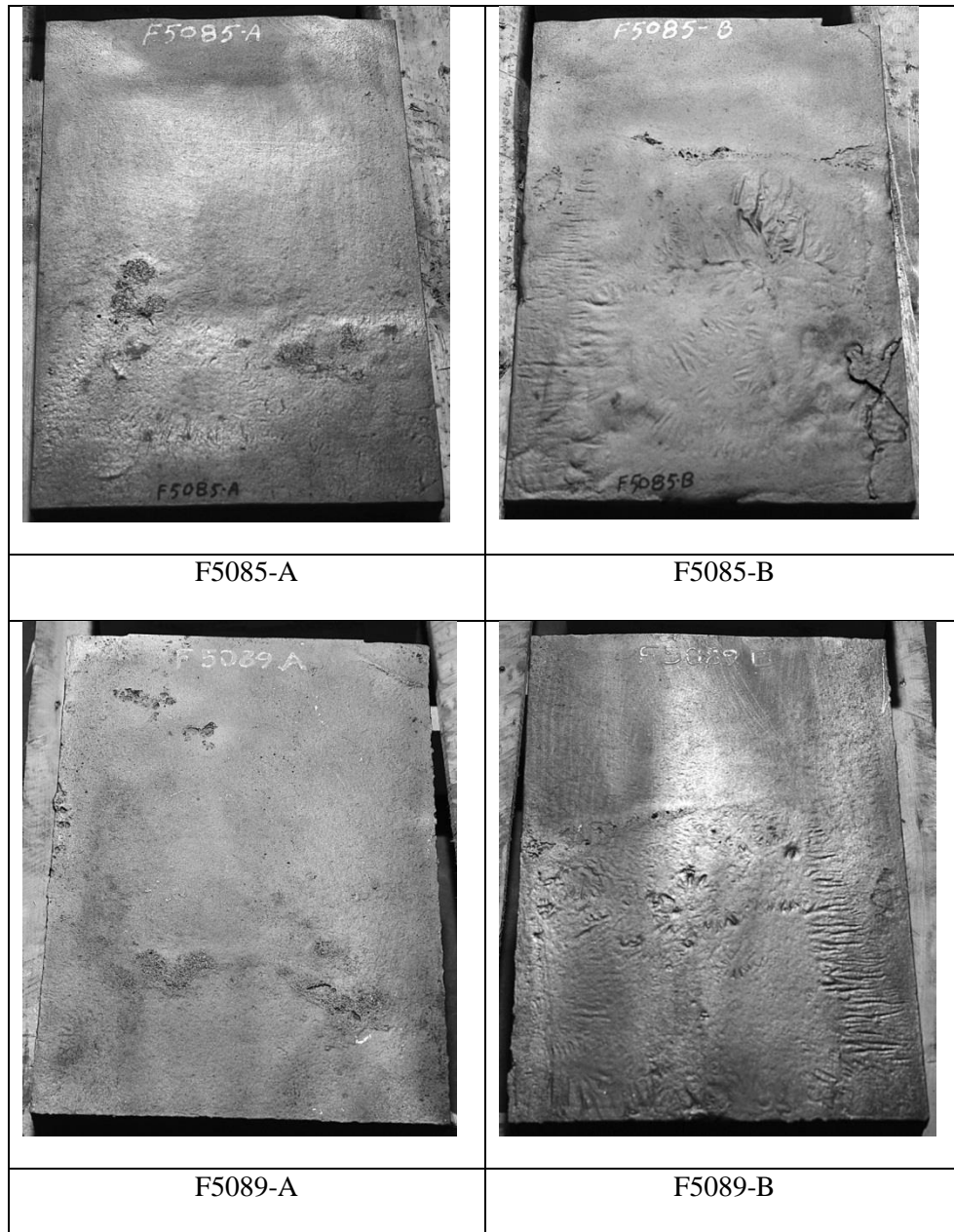
Figure 8 – Laboratory trials castings of heats F5085 and F5089. Steel AISI 1020 carbon steel was poured.

3.3.3 Industrial Trials

Industrial trials were conducted at Harrison Steel Company. The pour weight was about 9500 lb. Large spindle casting for an off-road vehicle was poured. Prior data existed for pouring cup and submerged pouring into side riser. Cleaner castings were obtained by submerged pouring into pouring basin.

Pouring basin allows for a choked design in bottom-pouring and also is a lower cost option. The gating system is partially shown in Figure 9.
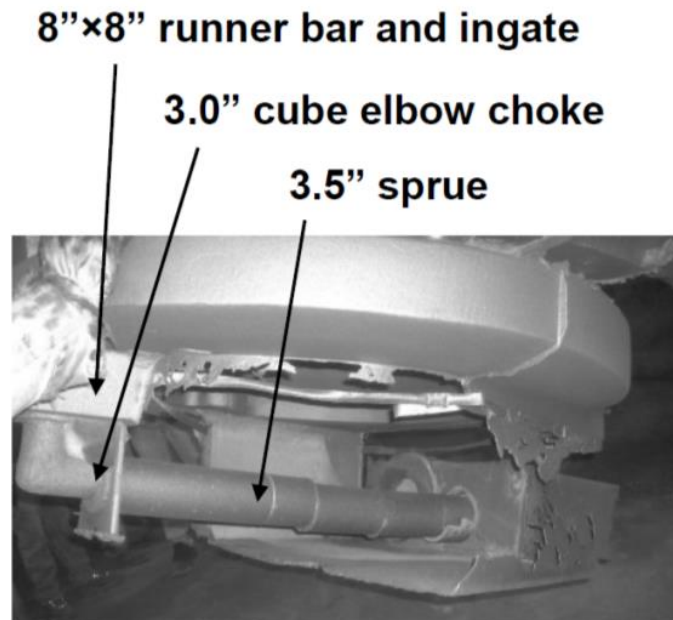
Figure 9 – Casting tress from industrial trials at Harrison Steel Company.

3.4 TASKS 4– Gating Designs and Flow Simulation Using Magma Software

3.4.1 Gating Designs for Automotive Turbo-Housing Stainless Steel Castings

Gating design has received much attention to the casting cleanliness, inclusions, oxide films, and other defects. There are 10 criteria for casting gating design: (1) rapid mold filling, (2) minimizing turbulence, (3) avoiding mold and core erosion, (5) removing slag, dross, and inclusions, (6) promoting favourable thermal gradients, (7) maximizing yield, economical gating removal, (8) avoiding casting distortion, (9) compatibility with existing modeling/pouring methods, and (10) controlled flow conditions. Some desirable considerations often conflict with another desirable effects. A gating design system will generally be a compromise among conflicting design considerations, the final design being determined by the specific casting and its molding and pouring conditions.

In this work, a turbo housing pattern of Wescast was chosen to investigate the effect of gating design on the mold filling. Six gating designs were made and tested on the same casting. The gating area ratios are shown in Table 3 and the created CAD files are shown in Figure 10. Alloy (25Cr-13Ni stainless steel),

pouring temperature (1600°C), and other boundary conditions were the same for each gating modeling. The modeling outputs are temperature and velocity in the gating system.

Table 3 – Basic information about the six gating designs for Magma modeling

ID	Gating Description	Area Ratio (down spruce: runner: total ingates)
Gating 1	Current trial	1: 1: 1.7
Gating 2	Non-pressurized	1:1.7: 2.2
Gating 3	Partially Pressurized	1: 1: 0.75
Gating 4	Naturally pressurized	1: 1: 2.3
Gating 5	Naturally pressurized, without filter	1: 1: 2.3
Gating 6	Radial Choke Gating, without filter	1: 3: 3
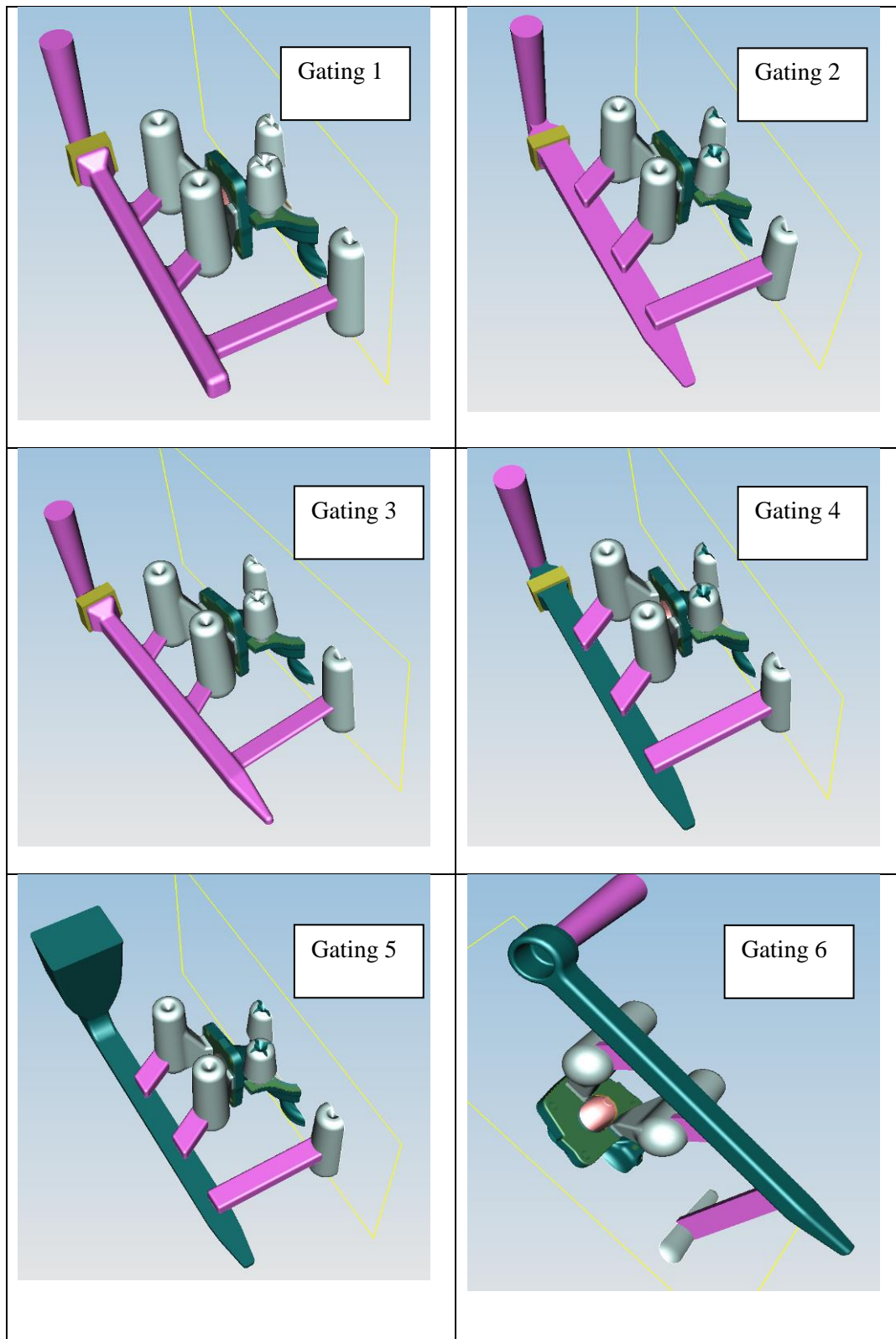
Figure 10 – Six gating designs for Magma modeling.

3.4.2 Mold Filling Simulation Using Magma Software

Figure 11 shows the simulation full view of mold filling for the six gating designs. Liquid metal temperature and velocity can be determined from the full views. Figure 12 shows the ingate temperatures at 4.5 sec into filling in different gating designs. The temperature variations within the three ingates are comparable or even larger than the temperature variations between the gating designs. The temperatures from 1.5 to 4.0 sec were also reviewed. From statistical ANOVA testing in Figure 13, there is no significant difference in the heat loss among the six gating designs with 95% confidence ($p > 0.05$).

Figure 14 presents the ingate velocity pictures at 3 sec filling. In addition, Figures 15, 16, and 17 illustrate the ingate velocity at 2, 3, and 4 sec during the mold filling, respectively. Gating 3 (pressurized gating) has a much faster ingate velocity than the rest of the gating designs. There is significant difference in the ingate velocity among the gating designs, as shown in the statistical testing results (Figure 18). The preferable filling velocity should be less than 1 m/s. Therefore, Gating 3 seems unfavourable for turbulence control and casting quality.

The current gating (Gating 1): The liquid metal enters the ingates before the entire runner is filled as shown in Figure 19, because the ingates are located in drag and they are slightly non-pressurized. Therefore, the metal may enter the ingates and casting cavity prematurely.

Gating 6: The ingate velocity is low.

Gatings 2, 4, and 5 appear more favourable for mold filling. The entire runner fills before the metal rises to the level of the ingates.

According to the Magma modeling results, Gating 3 appears unfavourable, and Gatings 2, 4, 5, and 6 are more favourable. Gating 5 Magma is still under re-running with rectangular down sprue. The riser well depth is reduced to typical ½ D (D-riser diameter), since Magma results showed turbulence due to a deep riser well, especially the riser away from down sprue. The runner extension can be increased to further slow the liquid metal and catch the first metal.
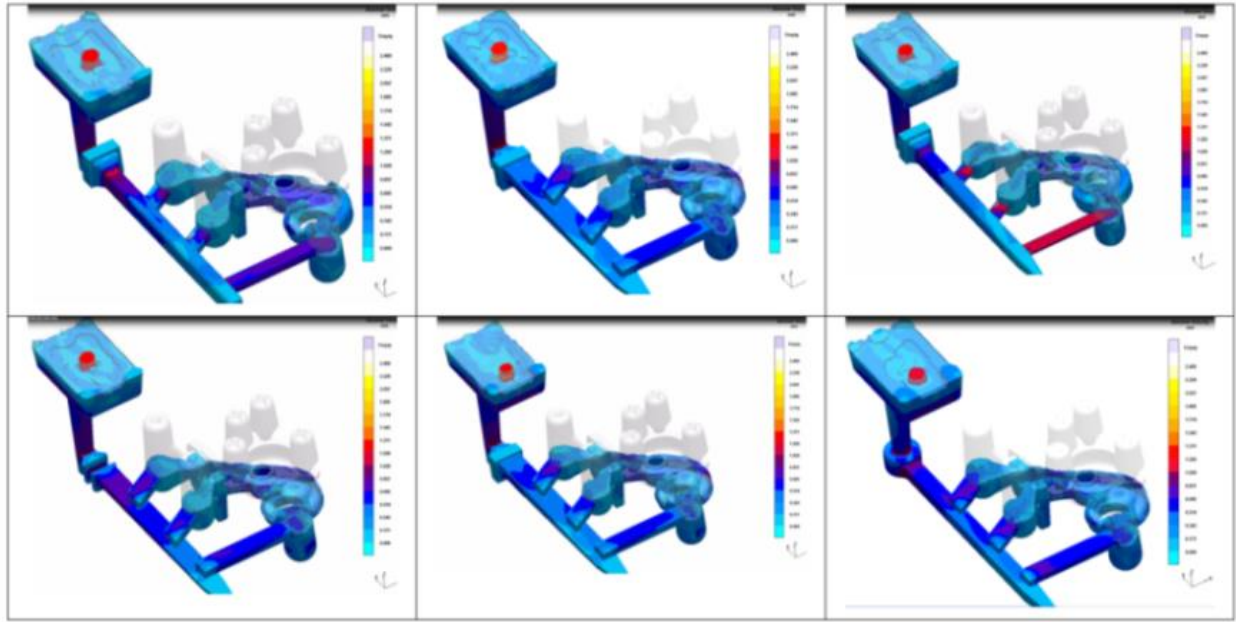
Figure 11 – Flow computer modeling full view using Magma for six gating designs to the same pattern.
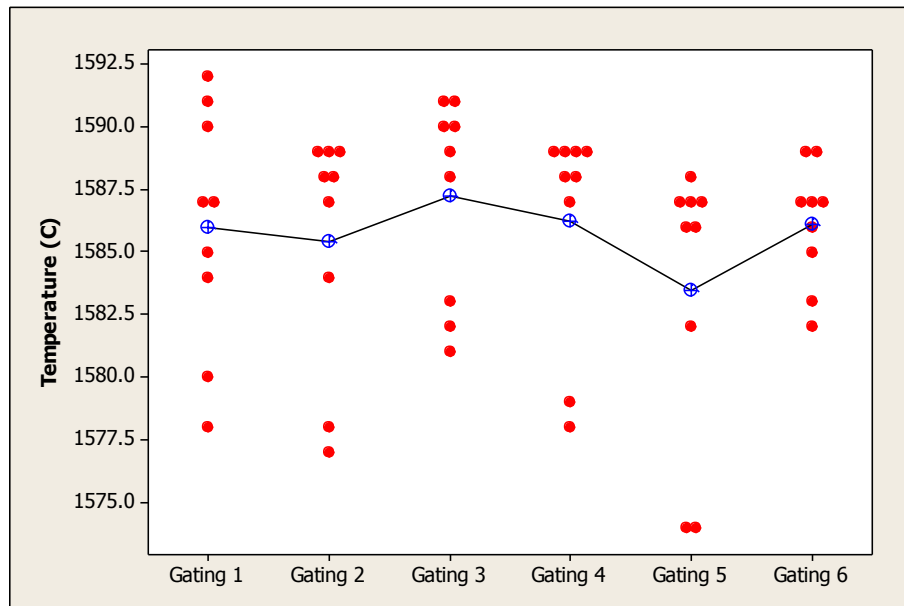
Figure 12 – Ingate temperature at 4.5 sec mold filling.

```
Source   DF       SS    MS     F      P
Factor    5     71.9  14.4  0.72  0.609
Error    48    954.4  19.9
Total    53   1026.4
S = 4.459   R-Sq = 7.01%   R-Sq(adj) = 0.00%

                           Individual 95% CIs For Mean Based on
                           Pooled StDev
Level      N    Mean  StDev  --------+---------+---------+---------+-
Gating 1   9  1586.00   4.80                (-----------*-----------)
Gating 2   9  1585.44   4.77            (-----------*-----------)
Gating 3   9  1587.22   4.06                   (-----------*-----------)
Gating 4   9  1586.22   4.44             (-----------*-----------)
Gating 5   9  1583.44   5.61   (-----------*-----------)
Gating 6   9  1586.11   2.42             (-----------*-----------)
                           --------+---------+---------+---------+-
                              1582.5    1585.0    1587.5    1590.0
```
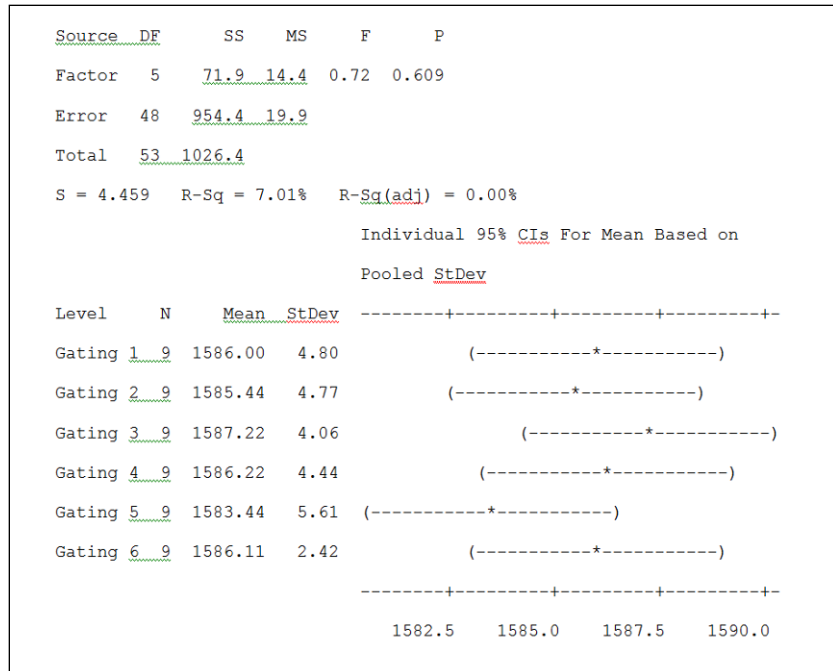
Figure 13 – ANOVA (Analysis of Variance) testing of ingate temperatures at 4.5 s filling.

25
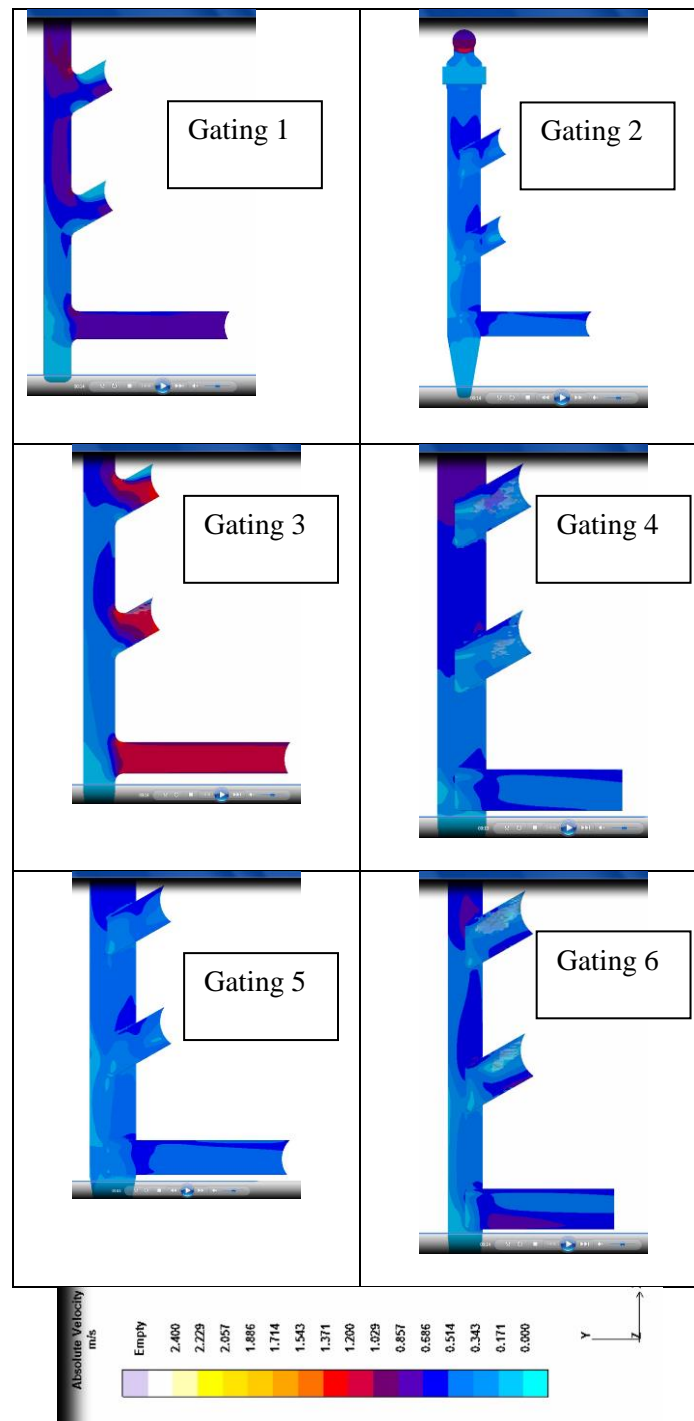
Figure 14 – Ingate velocity pictures at 3 sec mold filling.
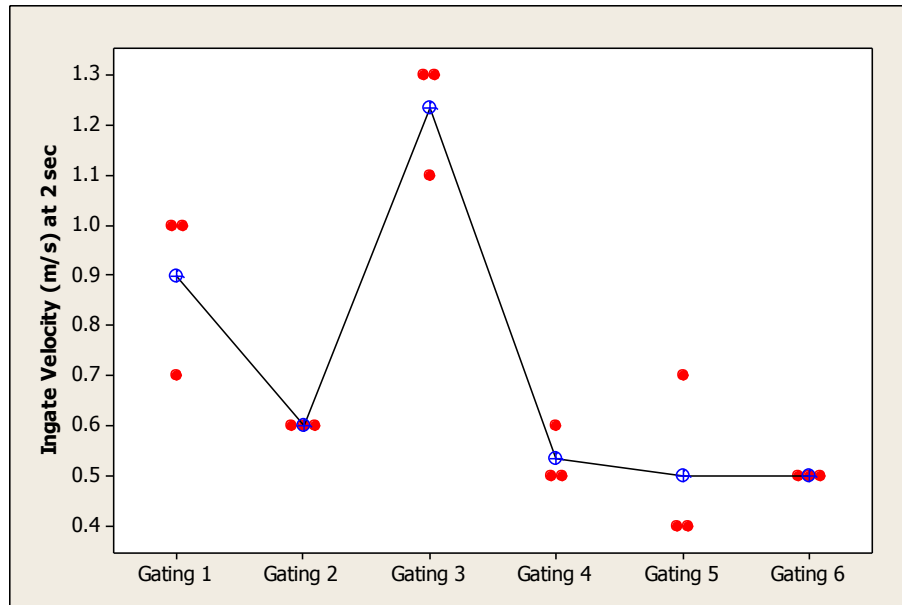
Figure 15 – Ingate velocity at 2 s mold filling for the six gatings.

Figure 16 – Ingate velocity graph at 3 sec mold filling.

Figure 18 – Ingate velocity graph at 4 sec mold filling.

Figure 18 – ANOVA testing of ingate velocity at 3 sec mold filling.

Figure 19 – The filling picture of Gating 1 (current pattern): early metal enters ingates.

3.5 TASKS 5– Industrial Trials of Producing Turbo-Housing Stainless Steel Castings
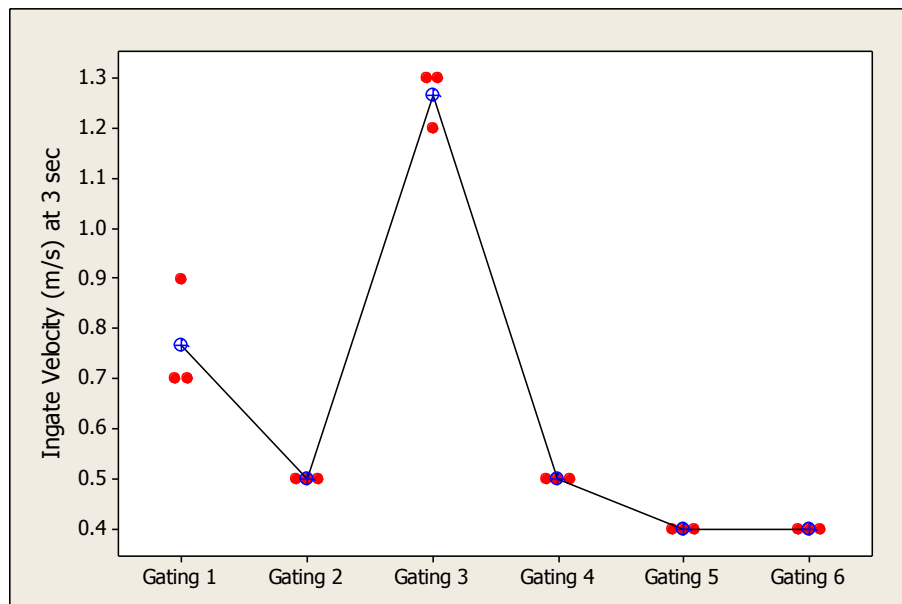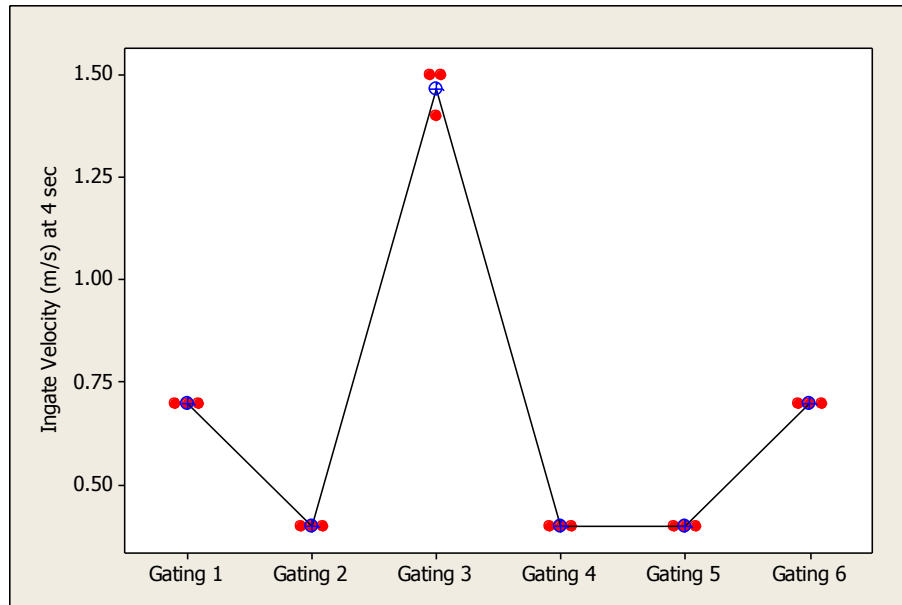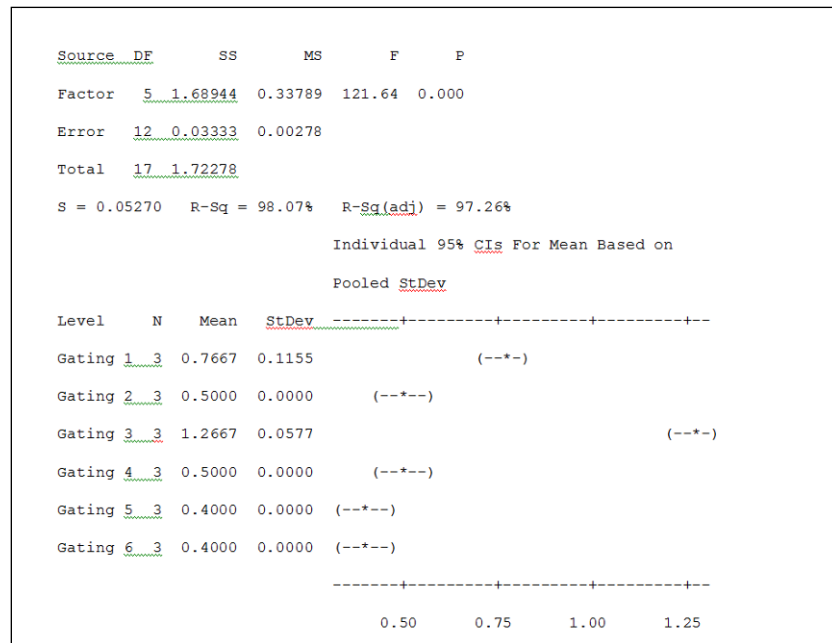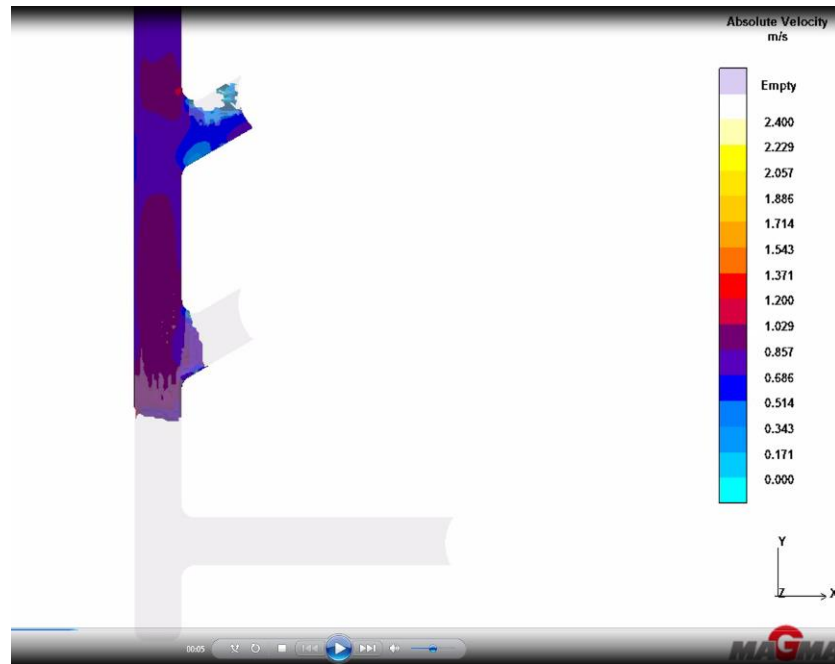
3.5.1 Casting Trials of Stainless Steel Turbo-Housings

Based on the simulation results, three gatings were selected for casting trials, including partially pressurized gating (G3), naturally pressurized gating (G4), and radial choked gating (G6). The melting and casting trials were performed on August 2nd, 2013, at Wescast Industries Inc. Brantford, Ontario. The stainless steel alloy for the trials was: 1.4837 (or HH grade 13%Ni and 25% Cr). Charges of 600 lbs. were melted and lip poured. A prototype turbo-housing tooling was chosen for the casting trials. Three castings were produced for each gating condition. Figures 20, 21, and 22 are the gating pattern pictures for the trials. Figures 23 and 24 are the mold pictures (9 molds in total), before and after pouring.

Table 4 lists the stainless steel chemistry from ladle samples, which is within the specification of ASTM A297. Table 5 summarizes the trial recorded information and casting review results. It is seen from Table 5 that (1) Gating 3 without filter had the worst casting quality, and (2) Gating 6 (radial choke) improved the casting yield without slowing down the pouring time. For example, Figure 25 presents the casting comparisons. If no filters were used, radial-choke gated casting showed casting cleanliness improvements. The small web thickness of the radial-choke gating significantly reduced the Reynold's [Re] number (Equation 1 in this report) and thus lowered the flow turbulence. The casting shrinkage was reduced by lowering the pouring temperature to a certain extent.

| Cope | Drag |

Figure 20 – Pattern pictures of pressurized gating (G3).

| Cope | Drag |
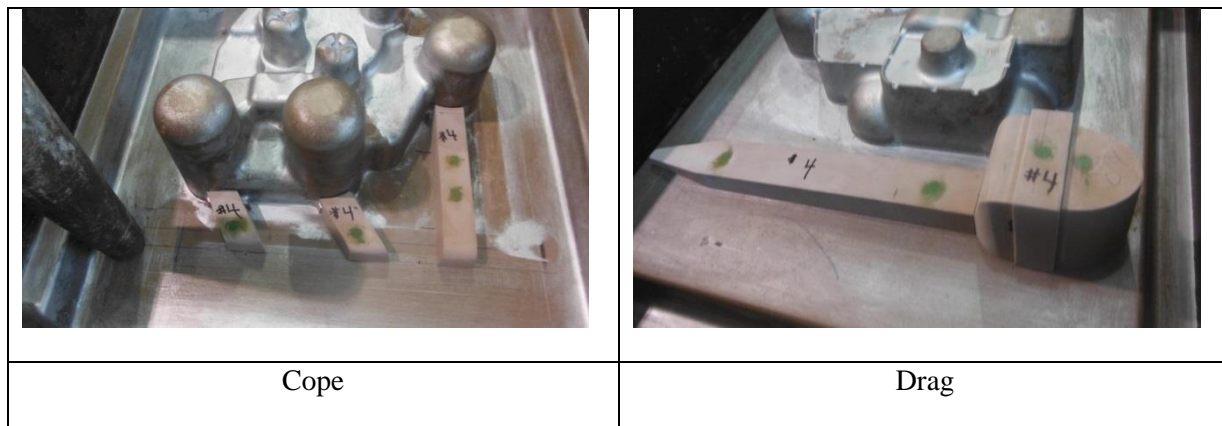
Figure 21 – Pattern pictures of naturally pressurized gating (G4).

| Cope | Drag |
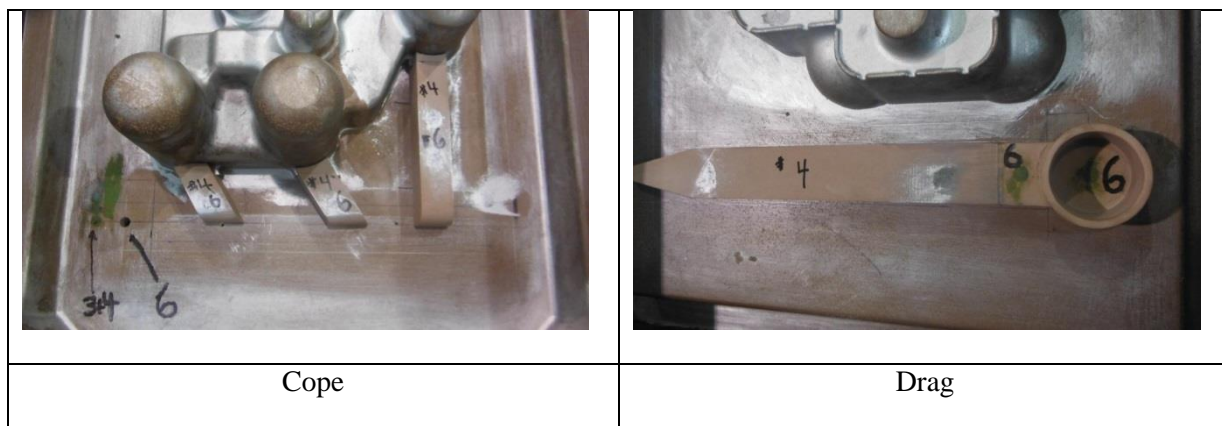
Figure 22 – Pattern pictures of radial choked gating (G6).

Figure 23 – Nine molds prior to pouring.

Figure 24 – Nine molds just poured.

Table 4 – Stainless steel from ladle sample (wt.%)

C	Si	Mn	Cr	Ni	P	S	Nb	Fe
0.40	1.20	0.80	24.90	13.90	0.03	0.11	0.97	~57

Table 5 – Trial recording and casting review

| Mold ID	G3- no filter	G4- filter	G6- no filter	G6- no filter	G3- filter	G4- no filter	G4- no filter	G6- no filter	G3- no filter
Pour Order	**1**	**2**	**3**	**4**	**5**	**6**	**7**	**8**	**9**
Pour Temp, F	3024					2944			2844
Pour Time, s	6.75	11.06	6.5	6.56	7.22	5.59	6.09	5.69	
Tree weight (lb)	45.2	47.2	41.9	41.4	44.8	47.10	46.50	41.80	45.1
Drag surface	rough	rough	rough	rough	rough	less rough	less rough	rough	rough
Section	yes	no	tree kept	yes	no	yes	yes	no	yes
Fins	yes	yes	yes	yes	yes	yes	yes	yes	yes
Shrinkage	2 flanges	2 flanges		2 flanges	1 flange	little	1 flange	no	no
Incl. Outter	4 (~5 mm)	2 (<2 mm)	1 (<2 mm)	no	1 (~3 mm)	no	2 (~ 3 mm)	1 (<2 mm)	2 (~ 3 mm)
Incl. Inner	4 (~5 mm)	no	no	1 (< 2 mm)	1 (~5 mm)	1 (~5 mm)	No	no	no
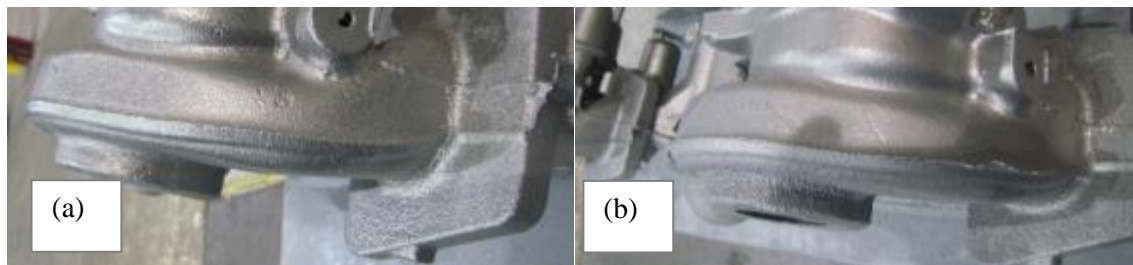
Figure 25 – Casting comparison: (a) casting #1 (partially pressurized, no filter) with inclusion defects observed and (b) casting #3 (radial choked gating, no filter) without inclusion defects.

3.5.2 Trial Casting Analysis

The floor layout of trial castings is shown in Figure 26 for review. Some castings were sectioned. In addition, metallographic samples were taken from casting #4, #7, and #9 (The ID is pouring order in Table 5), to conduct micro inclusion analysis using SEM. No filters were utilized in these three castings and they represented each gating condition.


Figure 26 – Nine trial castings layout on the floor for review

Figure 27 presents typical SEM micrographs for the three castings #4, #7 and #9. The microstructure consists of austenitic matrix, eutectic carbides, and inclusions. The size of these micro inclusions is in the range of 1 to 5 μm. The volume fraction of micro inclusions was determined to be approximately ~2%. There is no appreciable difference in the volume fraction of micro inclusions among the three castings.

Two major types of micro inclusions were observed, as shown in Figure 28: grey color and black color. They are Manganese sulfides and silicates, as identified by using SEM EDS. The sulfides are usually located in the vicinity of interdendritic boundary areas. The silicates are scattered within the matrix, as marked in Figure 28.

Figure 29 illustrates the micrographs of inclusions at higher magnifications. Interestingly, the sulfide inclusions consist of other, finer inclusions (Figure 29a). For example, the dark spots in Figure 29a were identified as silicates. In addition to Mn, Si, and oxygen, this sulfide includes appreciable contents of Fe and Cr. The silicate (Figure 29b) is surrounded by a layer of sulfides. In order to improve machining, the silicate amount should be reduced. This may suggest that the silicon content of the stainless steel should be controlled.

Casting # 4	Casting # 7
	Figure 27 – Typical SEM micrographs from three castings.
Casting #9	
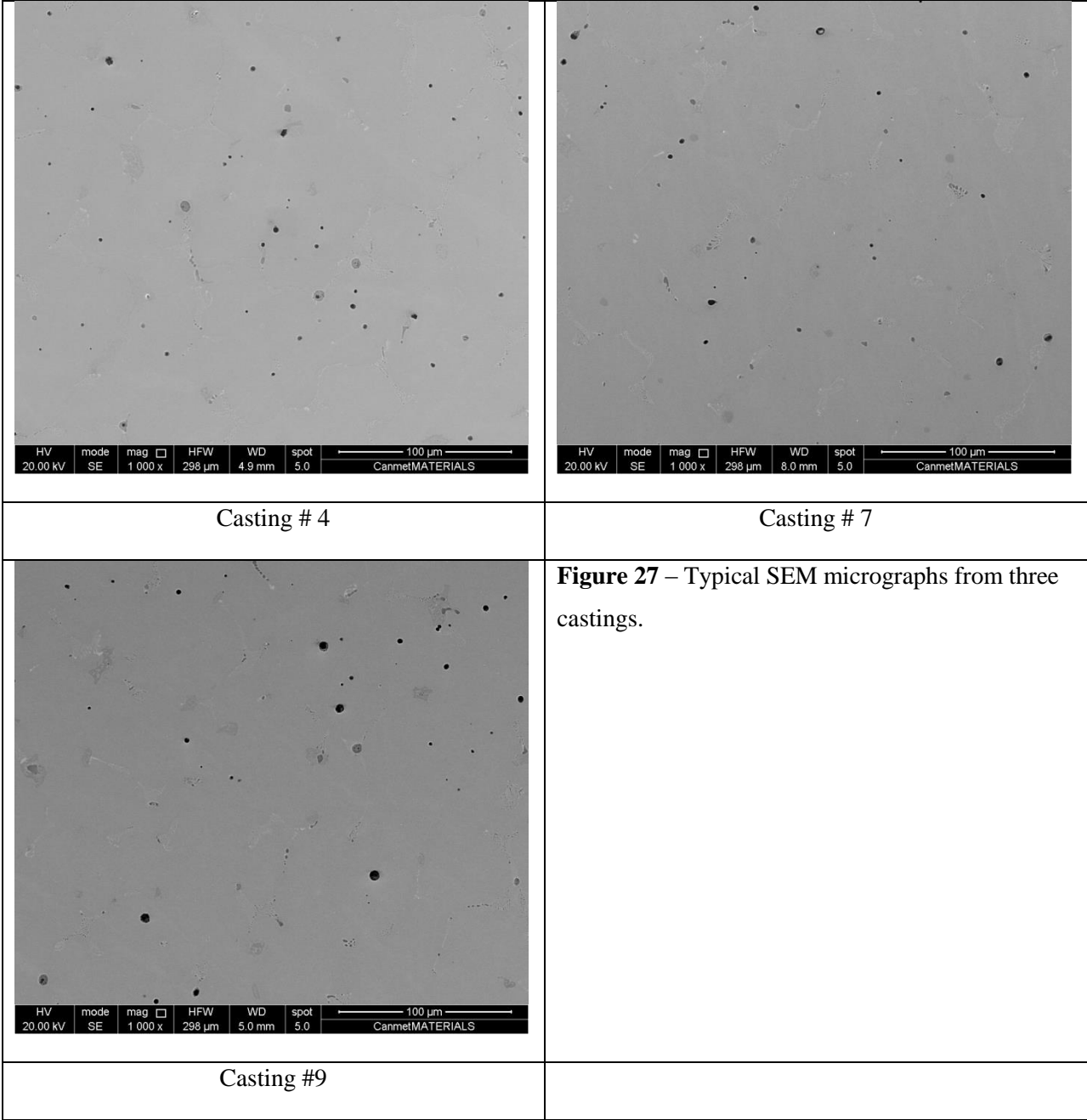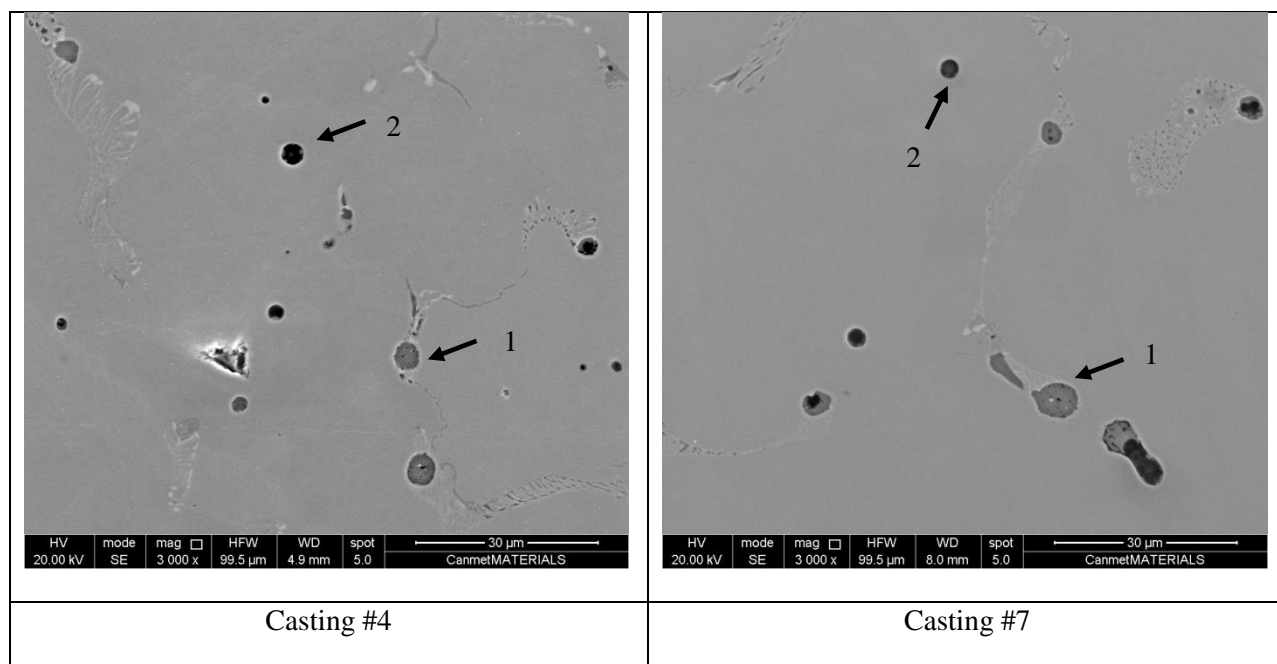
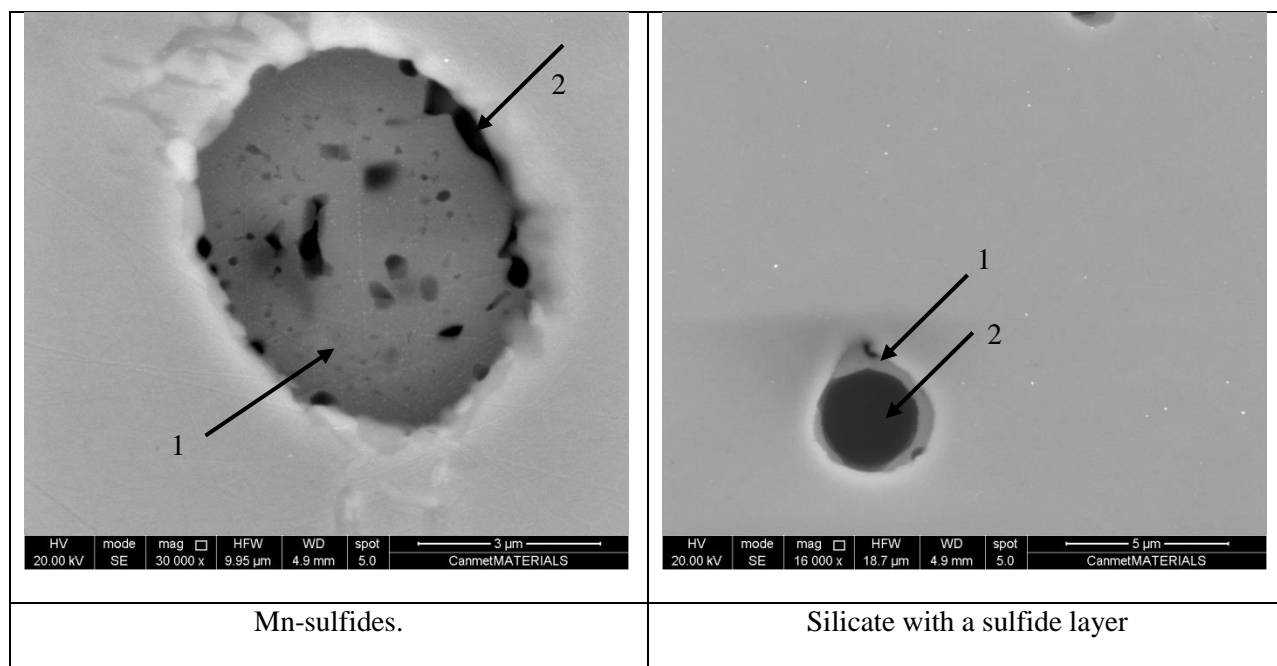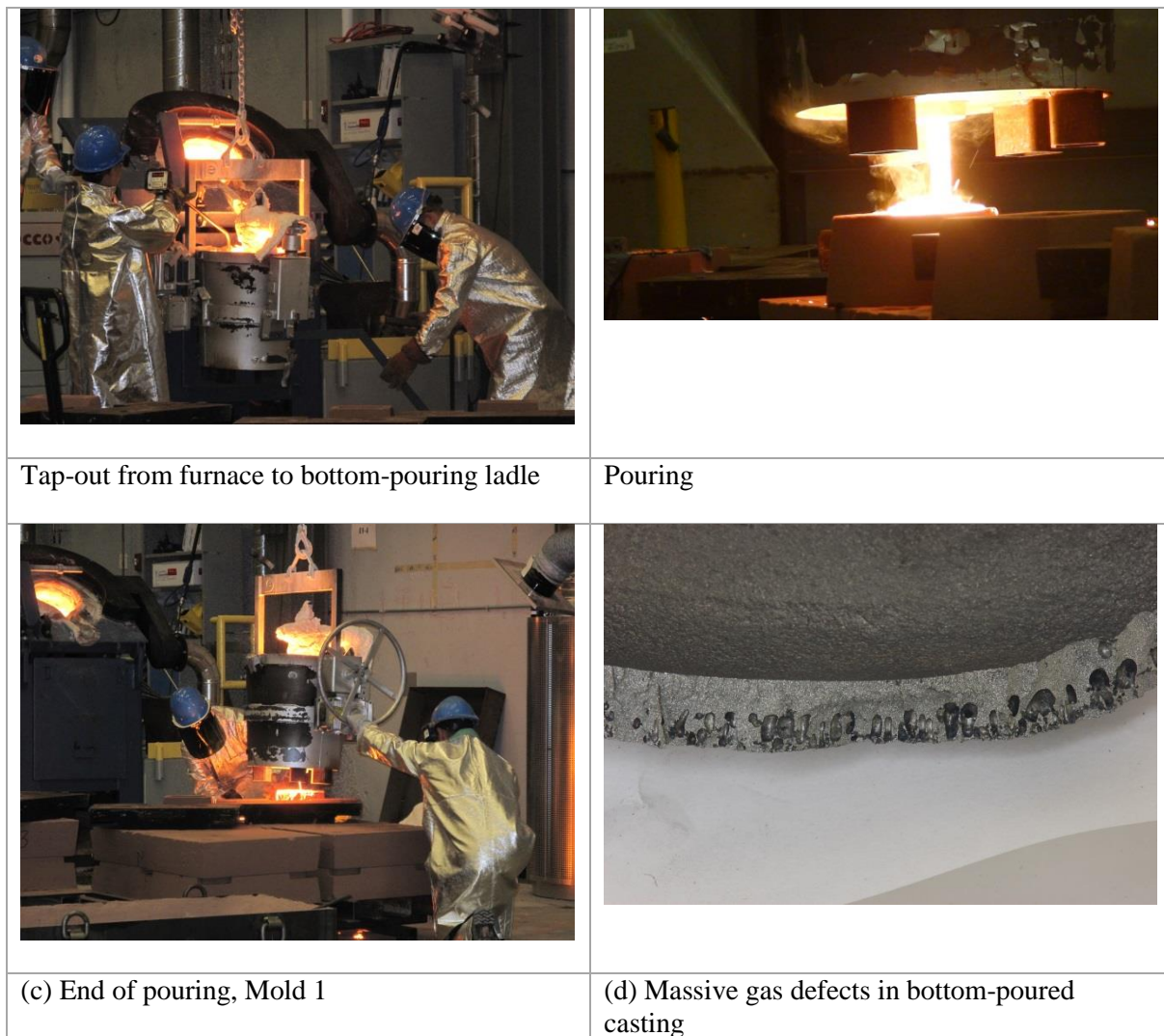**Figure 28** – Two major types of micro inclusions observed.   Arrow 1 points to sulfide inclusion in the grain boundary areas. Arrow 2 points to silicate inclusion within the matrix.

Figure 29 - Micrographs of sulfides and silicates under higher magnifications. Arrow 1 points to sulfides and arrow 2 points to silicates.

3.5.3 Bottom-pouring castings

In addition to using lip-pouring, bottom-pouring trials were performed for the automotive turbo-housing castings. The pictures of the experiment and the results are shown in Figure 30. Massive gas defects were observed with the casting (Figure 30d). These massive gas defects did not occur for the lip pouring, regardless of whichever gating system was used. As observed in the water simulation studies, bottom pouring can generate a huge amount of air entrainment. It was confirmed again that the least entrainment defects were formed from small, lip-poured ladles.

Tap-out from furnace to bottom-pouring ladle	Pouring
(c) End of pouring, Mold 1	(d) Massive gas defects in bottom-poured casting

Figure 30 – Bottom-pouring experiments on automotive turbo-housing castings at CanmetMATERIALS.

4 Benefits Assessment

The bottom-pouring with new basin designs (dam), submerged nozzle, and nozzle extension effectively improved the large steel casting cleanliness, as observed in industrial trials.

The lip-pouring trials of automotive castings showed the influence of gating on the stainless steel casting cleanliness. Radial-choke gating design resulted in the reduction of casting tree weight by 12%. The casting cleanliness was improved, as well. The radial-choked gating can produce clean steel castings without resorting to the ceramic filters in gating, which would have huge potential savings for the metalcasting industry.

5 Commercialization

The bottom-pouring new gating designs developed in this project included basin with a dam, submerged nozzle, nozzle extension, and downsprue choke. They are commercially available and have already been implemented at Harrison and Wescast foundries.

Radial choke gating showed casting yield and cleanliness improvements. Further confirmation trials in metalcasting companies are in progress.

6 Accomplishments

All of the five tasks were completed with several industrial trials to prove steel casting cleanliness improvements. There have been three published papers, presentations and a series of technical reports.

6.1 Published Papers

1) S. Kuyucak "Sponsored Research: Clean steel casting production - water modeling studies of bottom-pouring ladle operations", AFS Trans., Vol. 114, Paper No. 06-095, (2006).

2) S. Kuyucak, "Sponsored Research: Clean steel casting production - evaluation of laboratory castings", AFS Trans., Vol. 115, Paper No. 07-103 (2007).

3) Delin Li and Clayton Sloss, "Cast Ferritic Stainless Steels for Automotive Exhaust Components", AFS Proceedings 2013, Panel 13-1263 (2013).

6.2 Presentations

1) S. Kuyucak, "Sponsored Research: Clean steel casting production - evaluation of Industrial castings", 111th Metalcasting Congress AFS, Houston, TX, (May 15-18, 2007).

2) Delin Li, "Cast Ferritic Stainless Steels for Automotive Exhaust Components", AFS CASTEXPO & METALCASTING CONGRESS, AFS, April 6-9, 2013, St. Louis, Missouri.

3) Delin Li, "Gating Designs, Magma Simulation, and Industrial Trials of Stainless Steel Castings", presented at AFS Division 9 (Steel Casting) Conference Call, October 22, 2013.

4) Delin Li, "Effect of Gating on Stainless Steel Casting Cleanliness", to be presented at 118th AFS Congress, Schaumburg, IL, April 8-11, 2014.

7 Summary and Conclusions

A broad range of clean steel casting research has been carried out in this project, including bottom pouring and lip pouring, low alloy carbon steel and high alloy stainless steel, water simulation and computer modeling. Throughout this project, there have been effective collaborations among CanmetMaterials laboratory, industrial companies (Wescast Industries Inc., and Harrison Steel Company), and AFS. In summary, the following was concluded from the research project:

1) Air entrainment was demonstrated and measured for the bottom-pouring system using water modeling. On average 30% air by steel volume becomes entrained in a ladle bottom-pouring operation, which is the main cause of entrainments defects in steel castings.

2) New bottom-pouring designs consisted of a submerged ladle nozzle extension, pour basin, dam, and choked sprue at the sprue base. From the water modeling, the new designs resulted in significant reduction in air entrainment and flow turbulence in the gating system.

3) The new bottom-pouring designs were also tested in Canmet laboratory casting experiments on AISI 1020 carbon steel casting plates and industrial trials on a spindle castings,. Cleaner castings have been obtained by submerged pouring into a pouring basin.

4) From 2012- 2013, this project placed emphasis on the automotive turbo-housing stainless steel castings and lip-pouring process. Six gatings with different locations, area ratio, and shapes were designed for the same casting pattern to examine the gating influence on the steel casting cleanliness. Computer modeling using Magma software was completed and showed the melt velocity was significantly influenced by the gating. The temperature loss was not very sensitive to the gating designs.

5) Three gatings were chosen for melting casting experiments in Wescast Industries Inc., Brantford, Ontario. It was observed that (1) the pressurized gating (G3) had the most surface macro inclusions and (2) the radial choke gating had the least macro inclusions among the molds without gating filters.

In addition, the radial-choke gating improved the casting yield by 12%. The concept of radial choke gating was introduced by AFS through this project.

6) Metallographic specimens were prepared from three trials castings that were produced without mold filters. SEM analysis indicated that (1) the amount, size, and composition of the micro inclusions are similar among the three specimens, (2) two major types of micro inclusions were identified, sulfides at interdendritic boundaries, and silicate within the matrix. In order to improve machining of stainless steel castings, a certain amount of sulfides can be beneficial and silicate inclusions should be minimized.

8 References

1) ASM Handbook, Volume 15, Casting, 4th printing, March, ISBN 0-87170-007-7, Chapter "Inclusion-Forming Reactions" by Paul K. Trojan (University of Michigan-Dearborn), 1998.

2) John Campbell, "Complete Casting Handbook: Metal Casting Process, Metallurgy, Technical and Design", Elsevier Ltd., ISBN-13: 978-1-85617-809-9, 2011.

3) Daniel E. Groteke, "A Sprue and Well Redesign for Aluminum Sand Molding" Q. C. Designs Inc. report, 2012.

4) George Goodrich (technical editor), "Casting Defects, AFS Handbook: Iron & Steel", ISBN 978-87433-314-5, AFS, 2008.

5) R.W. Monroe, and M. Blair, "Steel Foundry Research", WFO (World Foundry Organization) Tech Forum, St. Louis, MO, April 19, 2005.

6) Malcolm Blair and Thomas L. Stevens (editors), "Steel Castings Handbook, Sixth Edition", SFSA and ASM International, ISBN 0-87170-556-7, 1995.